System Identification Test Using Active Members

Jay-Chung Chen*
Hong Kong University of Science and Technology, Kowloon, Hong Kong
and
James L. Fanson†
Jet Propulsion Laboratory, California Institute of Technology, Pasadena, California 91109

A modal test using active members as the excitation source has been performed on a test bed truss structure representative of a portion of a large space system. Using the step sine testing technique, the frequency response functions are obtained and the modal parameters are extracted by the curve-fitting method. A total of 10 global modes and 3 local modes are obtained. The results are compared with those obtained by the conventional external excitation test.

I. Introduction

FUTURE space missions will require new methodology for controlling large space structures. The challenge lies in their extreme flexibility and/or extreme geometric shape accuracy requirements. Designing and testing these lightweight structural systems that maintain desired geometries when subjected to dynamic, thermal, and other environmental disturbances become a common enabling technology for many of the potential missions.

To meet these stringent on-orbit performance requirements, the structural systems can no longer be passive, i.e., merely providing strength and/or stiffness to react the loads. An active system, in which actuations are provided to compensate for the responses due to disturbances, becomes necessary to achieve the desired performance requirements. One common approach is to add the actuators and sensors onto passive structures and to synthesize an associated control scheme to compensate for the responses. Reaction jets and momentum wheels might be considered as actuators, and accelerometers and gyros as sensors. For large space structures, this approach results in an unacceptable increase in weight and volume. It will also cause the rigid body dynamics to tightly couple with the flexible body motions. This is undesirable since it is the structural flexibility that drives the mission requirements.

An alternative approach is to use internal force producing devices as structural members. All elastic deformation is carried through the load paths. By placing sensors and actuators in the load paths, the elastic motions of the structures can be measured directly and forces can be exerted in response to such deformation.

This is the concept of the active member, which functions as a conventional passive load carrying member as well as a sensor and an actuator. It measures only elastic motion and exerts only internal, self-equilibrated forces, thus decoupling the rigid-body dynamics from the flexible motion. Preliminary studies indicate that this approach is very effective for the control of large space structures.[1-9]

The structural dynamic characteristics of the system must be known a priori if efficient control is to be achieved. Usually, a test-verified analytical prediction will be used in the control design. Large space structures are deployed or erected in space to achieve their design configurations. Their extreme flexibility prohibits any testing on the ground in their mission configuration without an extraneous support system. On-orbit vibration testing provides not only the necessary dynamic characteristics for the control design but also the in situ, real-time data that may be used for other tasks such as the damage assessment by system identification.[10] Intuitively, the external force actuators can be used as the excitation sources for the on-orbit vibration test just as they are used in the ground test. The suitability of using internal force actuators for vibration testing has, however, not been investigated. The present study will describe a modal test on a truss structure for the purpose of system identification by using the dual purpose active members as the vibration sources. The active members are made of piezoelectric material, which provides micron level displacements by varying its electric field. The result of the modal test will be compared with that obtained by a conventional modal test, namely, using external shakers as the excitation source.

II. Description of Test Article and Active Members

The modal test was performed on the Precision Truss, which is shown in Fig. 1 with some of the testing equipment. The Precision Truss is so named because of the precision con-

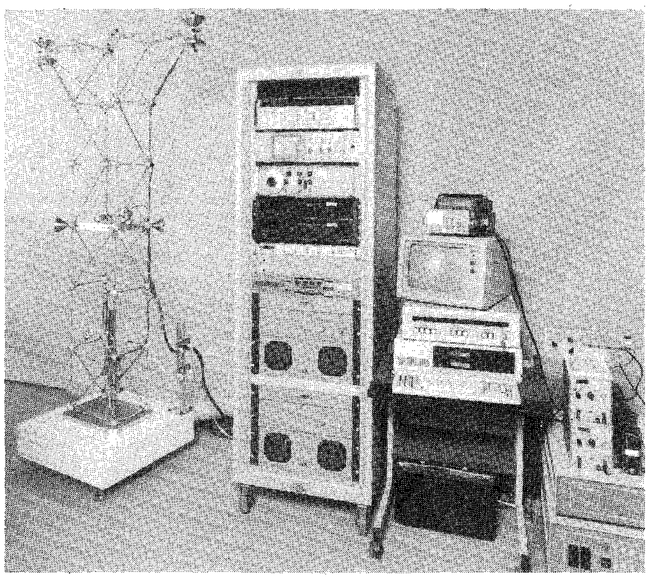

Fig. 1 Precision Truss and testing equipment.

Presented as Paper 89-1290 at the AIAA 30th Structures, Structural Dynamics and Materials Conference, Mobile, AL, April 3-5, 1989; received May 23, 1989; revision received May 8, 1990; accepted for publication May 12, 1990.

*Director of Research, Professor of Mechanical Engineering. Associate Fellow AIAA.

†Member of Technical Staff, Applied Technology Section. Member AIAA.

trol experiments planned for this test article. The six-bay four-longeron statically indeterminate truss is approximately 1.8 m (6-ft) tall and is built up of 0.635-cm- (0.25-in.) diam aluminum tube struts connected to 3.81-cm- (1.5-in.) diam aluminum joints. Each joint has a 26-hole pattern that can support a wide variety of truss geometries. Each strut is equipped with a custom-designed connector that allows it to be removed and replaced without disassembling the truss. In this way, active members can be retrofitted easily into any location on the structure. The base of the structure is cantilevered from a 0.61 × 10.15 m (2 ft × 6 in.) steel block weighing approximately 454 kg (1000 lb). The steel block rests on three jack feet placed on a concrete floor. The weight of the block on the support feet ensures a solid, low friction cantilevered boundary condition.

For a realistic simulation of the behavior of a large space structure, the presence of a large number of closely spaced, lightly damped, coupled modes must be incorporated into the test article. A rectangular cross section was chosen for the Precision Truss in order that two outriggers with concentrated masses could be added to tune the second bending and first torsional modes to have approximately the same frequency as the first bending mode. The frequencies of the second global bending and torsional modes was lowered approximately to a factor of three of that of the first set by adding rigid masses at the midspan section. This is a significant reduction in view of the fact that the second set of global modes occurs at frequencies six times higher than that of the first set for a uniform cantilevered beam. By properly adjusting the added masses, additional local modes were introduced between the frequencies of the first and second set of the global modes. Although it appears that the test article is too stiff to be representative of a real large space structure, the critical requirement of closely spaced modal frequencies has been fulfilled.

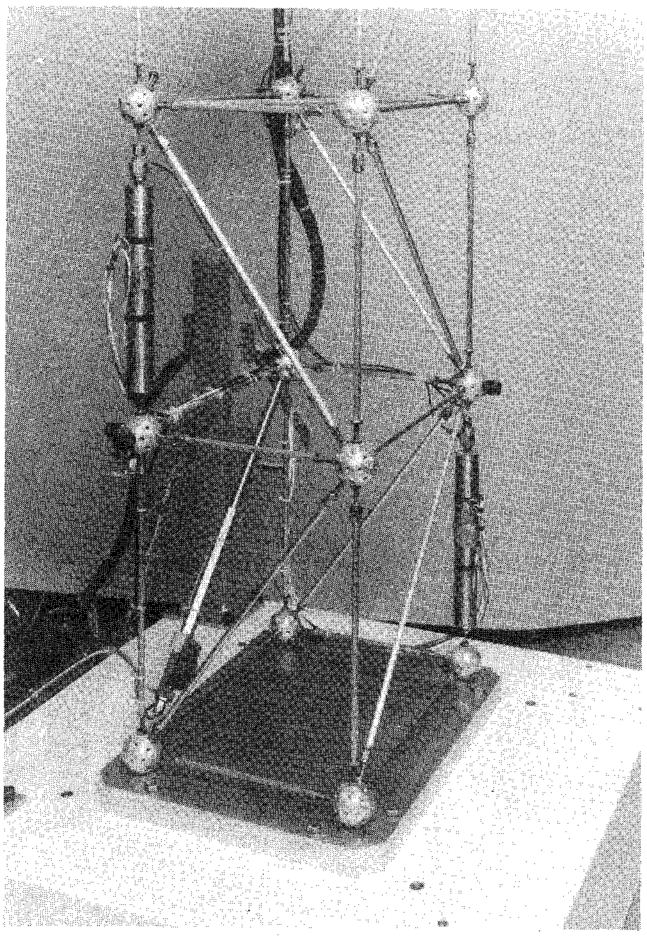

Fig. 2 Close-up of active members in Precision Truss.

Three active members were installed in the test article, two located in the lowest bay, one acts as a diagonal strut and the other as a longeron strut (strut 11). The third one is located within the next bay as a Longeron strut (strut 22). Figure 2 shows a close-up of these active members in the Precision Truss. These active members are made of a piezoelectric ceramic material that changes its strain when an electric voltage is applied. If the piezoelectric material is constrained when the voltage is applied, a force will be generated whose magnitude will be the function of the applied voltage and the compliances of the constraints and the piezoelectric material. Figure 3 shows such a relationship measured from the diagonal active member strut when it was placed in the calibration fixture and the voltage was applied quasistatically. Because the calibration fixture is relatively stiff, sufficient forces can be generated for very small strain. Figure 4 shows the force and displacement measurements as a function of the applied voltage for the longeron active strut when installed in the Precision Truss. The voltage was applied dynamically by a saw tooth periodic function. Again, it shows that sufficient force can be generated when the active members are integrated into the structure. It should be noted that both measurements show substantial amounts of hysteresis. By combining the two curves, it may show that the force displacement relationship appears to be linear. However, the hysteresis will be in the structural/control system since the applied voltage is an input/output quantity. The diagonal active strut is a commercial piezoelectric pusher and the longeron active struts are custom designed with a built-in displacement sensor. A more detailed description of these active members can be found in Ref. 11.

III. Modal Test Methodology

The test article was instrumented by 23 channels of accelerometers for the measurement of mode shapes. Additionally, load cell measurements were made at all three active members as well as displacement measurements for the two custom-designed active members used as longeron struts. Figure 5 shows the schematic of the test article in the modal test configuration with instrumentation locations and orientations indicated. The coordinates of the system, the three active members, and some of the grid numbers used in a NASTRAN analysis are also identified.

There are many modal test methods ranging from the classical sine dwell method, whose success is heavily dependent on the engineer's experience, to the various broadband excitation methods, which are highly automated.[12] The advantages and disadvantages of these methods were studied previously.[13] Since the objective of the present study is to investigate the feasibility of using active members as the exciting system for a

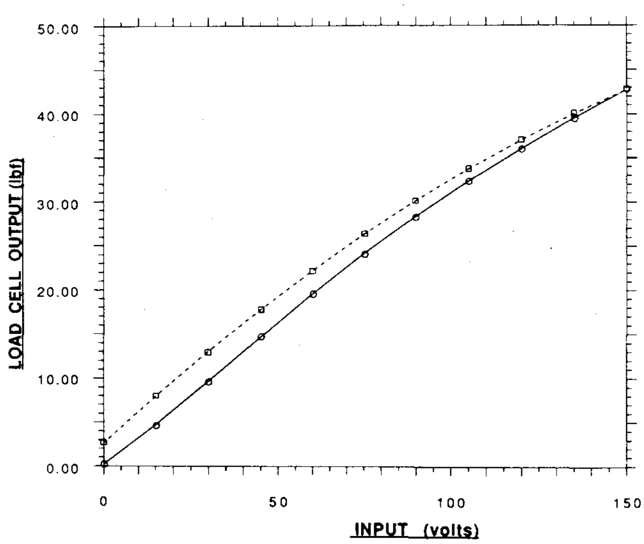

Fig. 3 Load-voltage relationship of diagonal active member strut.

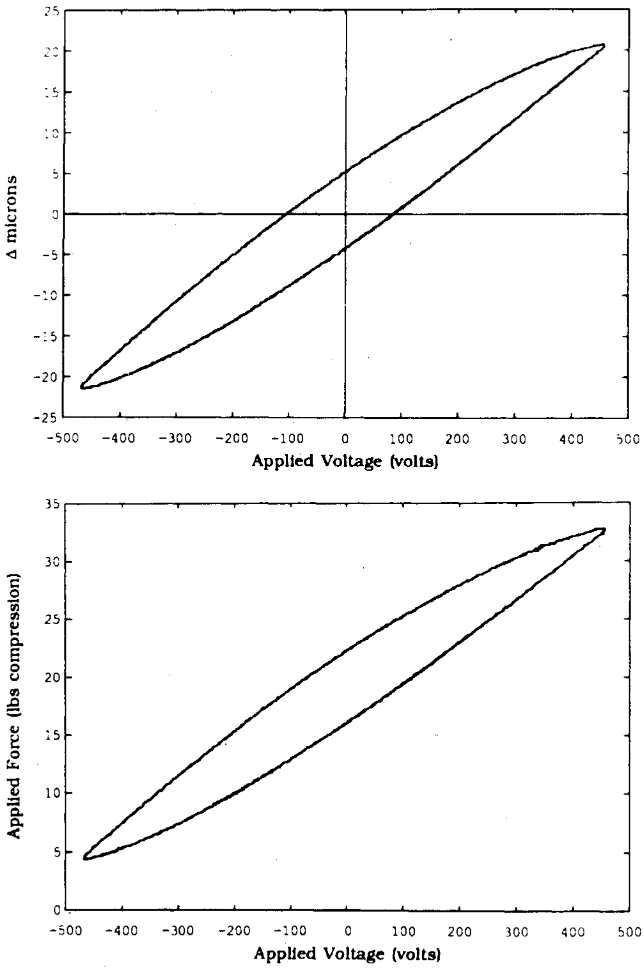

Fig. 4 Measured force and displacement as function of applied voltage.

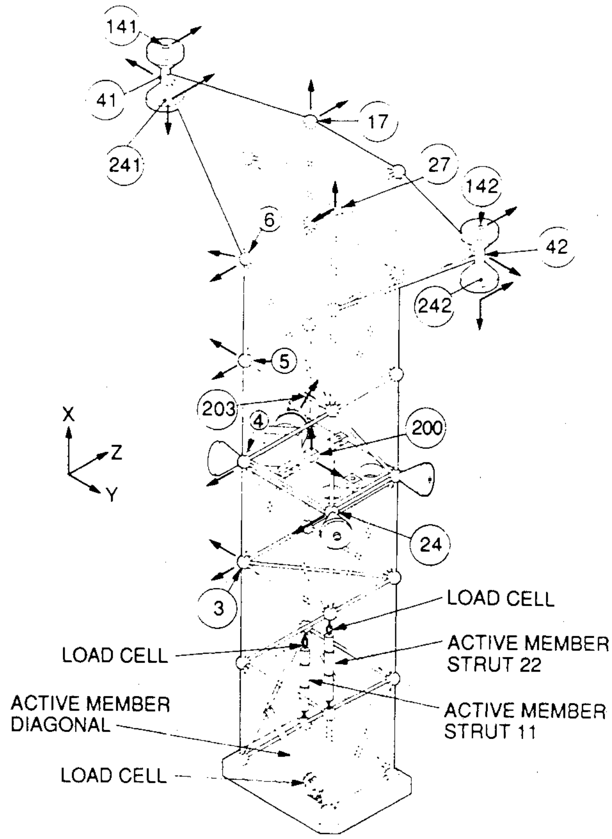

Fig. 5 Precision Truss in modal test configuration.

modal test, it is desirable that human factors be avoided in the comparison. The method chosen is the step sine technique.[14] In this method, the structure is excited by a single discrete frequency sinusoidal force and allowed to reach the steady state. The steady-state response time history is measured and averaged and its Fourier components are computed. The frequency of excitation is then stepped up by a small increment and the process is repeated until a predetermined frequency is reached. This discrete sine sweep test was conducted in two steps, one from 5 to 20 Hz, and the other from 20 to 60 Hz. The measured acceleration response spectra were integrated twice to obtain the displacement spectra, which are then divided by the excitation force to obtain the so-called frequency response function. Using a curve-fitting technique, the frequency, damping, and mode shape of the structure are extracted. The modal extraction procedure is performed using a commercial software package.

For purposes of comparison, the first modal test was conducted by using the conventional external shaker as the excitation source. A 45.4-kg (100-lb.) force electromechanical shaker was attached to the structure via a stinger that consists of a flexured rod, a load cell to measure the applied force, and a reference accelerometer to measure the response at the input point. A representative setup is shown in Fig. 6.

During the active member modal test, the external shaker was disconnected and a sinusoidal voltage was applied to the designated active strut. The displacement spectra are obtained in the same way as in the external shaker modal test. However, the frequency response functions are obtained by dividing the displacement spectra by the input voltage instead of the force measured by the load cell, which was located in series with the active member. The reason for this will be explained later. During the test, each of the active members is used as the excitation source one at a time. The active members not used as excitation sources remain passive. Since the piezoelectric ceramic material is relatively weak in tension, a biased dc voltage is applied to the active members at all times to assure the compression.

IV. Comparison of Test Results

First, the response levels due to the active member excitation are compared with that due to the external excitation, as shown in Fig. 7 for the acceleration response spectra at grid 5, direction Y. The vertical scale of Fig. 7 is in milligrams. This is a typical comparison that shows a higher response level for the external excitation. It also indicates that similar response levels can be achieved using the active member excitation at certain frequencies. The main reason for the low-level response is due to caution of not overloading the active members.

Next, the quality of the curve fitting will be examined. The curve fittings are performed in two frequency ranges, one from 5 to 20 Hz and the other from 20 to 60 Hz. A total of 10 global modes are identified: 3 modes in the low-frequency region and 7 modes in the high-frequency region. Additionally, 3 local modes are also identified. The individual channel comparison is shown in Fig. 8, which indicates that good quality curve fitting exists for all of the tests regardless of the type of excitation and the response levels. Each of the plots in Fig. 8 contains two parts; the top one is the phase angle comparison whose vertical scale is a linear angle between 0 and 360 deg, the lower one is the displacement spectra comparison whose vertical scale is in inches.

Frequency and Mode Shape

Based on the curve-fitting results, the extracted modal parameters such as the natural frequencies and dampings are summarized in Table 1. The modal frequencies are in very good agreement for all of the extracted modes regardless of the type of excitation used. However, the extracted modal damping values show discrepancies for the different tests. There are missing modes from the tests using the two longeron active members, namely, struts 11 and 22. These modes are omitted on purpose due to low response level and high noise level. The omission assures the quality of the other extracted modes. Because of similar response levels, the results of the diagonal active member excitation test will be used for comparisons. Tables 2 and 3 list the mode shape comparisons for modes 1 and 4, respectively. The mode shape at each grid is expressed by the direction of the motion (Dir) as defined in Fig. 5 and its displacement (Disp.). The modal amplitudes are normalized in such a way that the maximum value is unity. The phase angles are also normalized with respect to the value where maximum modal amplitude is measured so that the phase angle associated with the maximum modal amplitude is zero. Also, the modal amplitudes are listed in the order of their magnitudes such that not only the amplitudes can be compared but also their order can be compared. Comparison of mode 1 indicates that the modal amplitudes, their orders, and the phase angles are very close. Indeed, the two mode shapes are almost identical. It should be noted that the phase angles are all very close to 0, 180, or 360 deg. This means that the response is either in phase, i.e., 0 or 360 deg, or is out of phase, i.e., 180 deg, with respect to the reference measurement. This is defined as the phase coherence, which is one of the fundamental criteria of resonance for a linear elastic system with modal damping. The comparison of mode 4 indicates otherwise; except for the first five largest modal amplitudes, there is no agreement for the other measurements. Also, the phase coherence was not observed for those measurements. It appears that the phase coherence criterion can be used to judge the quality of the extracted modes. Figure 9 shows the Fourier components plot of the modal amplitudes in which the input force is real and each modal amplitude is one

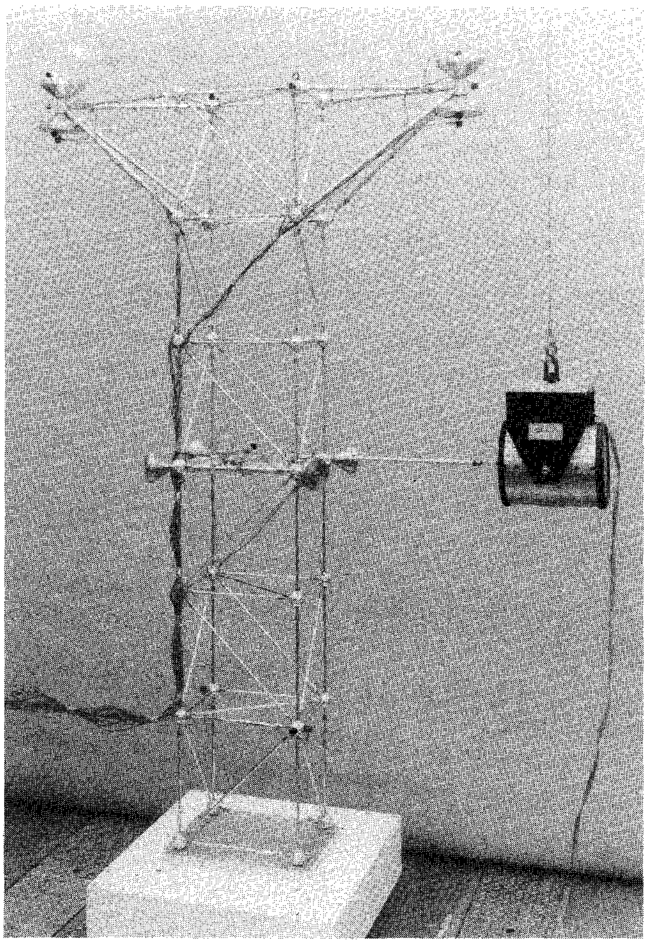

Fig. 6 External excitation.

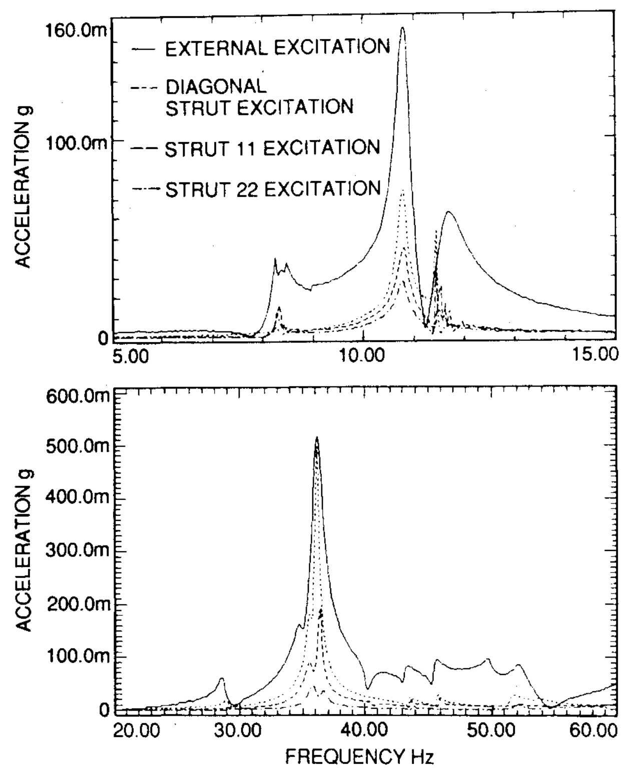

Fig. 7 Acceleration response levels at a representative node (node 5) due to different sources of excitation.

Table 1 Frequency and damping summary

	Frequency, Hz					Damping				
		Excitation method				Excitation method				
Mode	NASTRAN	Exernal	Strut 11	Strut 22	Diagonal	External	Strut 11	Strut 22	Diagonal	Description
1	8.189	8.253	8.312	8.274	8.291	0.0045	0.0037	0.0034	0.0018	Bending in Z
L1	7.372	8.785	——	——	8.815	——	——	——	——	Midbay shaker mass
2	10.722	10.747	10.791	10.773	10.770	0.0086	0.0119	0.0127	0.0102	Bending in Y
3	11.319	11.441	11.508	11.442	11.437	0.0009	0.0019	0.0009	0.0008	Torsion
L2	——	25.097	——	——	25.376	0.0024	——	——	0.0019	$-Y$ dumbbell rotation
L3	——	26.142	——	——	26.422	0.0035	——	——	0.0021	$+Y$ dumbbell rotation
4	——	28.662	29.795	——	29.014	0.0093	0.0077	——	0.0076	Y bending and boom walking
5	37.298	34.836	35.539	35.734	35.526	0.0086	0.0090	0.0079	0.0068	2nd Z bending
6	34.987	35.975	36.326	36.624	36.128	0.0040	0.0045	0.0061	0.0045	Y bending and boom walking
7	38.840	40.142	40.496	40.937	40.976	0.0049	0.0041	0.0049	0.0051	Z bending and torsion
8	——	43.227	43.587	43.828	43.576	0.0057	0.0023	0.0021	0.0028	$-Y$ boom in X
9	——	45.458	45.867	——	45.727	0.0043	0.0020	——	0.0025	$+Y$ boom in X
10	——	52.533	——	52.151	51.572	0.0062	——	0.0050	0.0082	2nd torsion

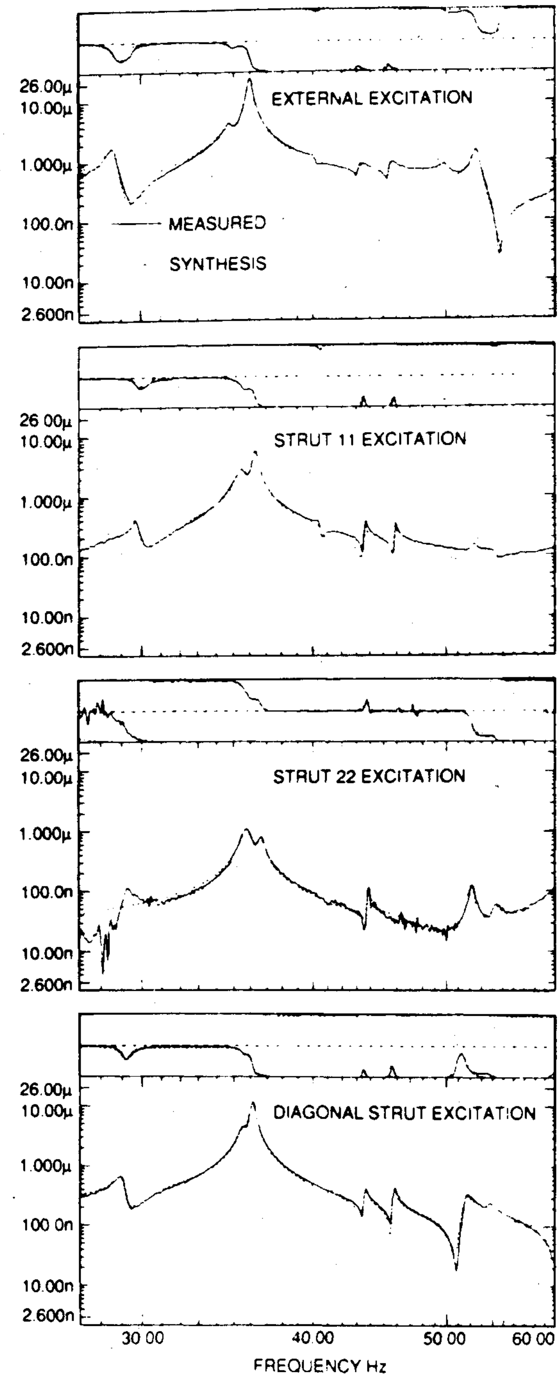

Fig. 8 Frequency response function comparison for grid 5Y.

point in this complex plane. Figure 9a is from mode 1, which shows that only one amplitude of any significance is slightly out of phase with respect to the rest of them. Referring to Table 2, it can be seen that grid 203, which is at the midbay shaker mass, was the one with slightly out of phase coherence. This particular measurement was troublesome throughout the test. Based on the phase coherence criterion, mode 1 is considered to be a high-quality mode. Figure 9b is from mode 4, which has bad phase coherence for most of its modal amplitudes; indeed, it is a low-quality mode. Figures 10 and 11 show the phase coherence for the 10 global modes. Only modes 4, 8, and 9 from the external excitation reveal poor phase coherence. It is interesting to note that the modes excited by the active member achieve better phase coherence.

Local Modes

A preliminary study indicates that there are three local modes. Mode L1 is the midbay shaker mass in motion only.

Table 2 Mode 1 comparison

Degree of freedom		External excitation			Active member excitation		
Grid	Dir.	Disp.	Phase	Order	Disp.	Phase	Order
142	Z	1.000	0.0	1	1.000	0.0	1
242	Z	0.901	359.7	2	0.896	359.8	2
27	−Z	0.863	179.8	3	0.853	180.0	3
17	Z	0.802	359.1	4	0.799	359.0	4
141	Z	0.790	358.3	5	0.783	358.0	5
203	——	0.736	327.9	6	0.528	343.3	8
241	Z	0.682	358.4	7	0.679	358.7	6
6	−Z	0.612	179.5	8	0.611	179.3	7
6	−Y−Z	0.486	180.0	9	0.478	179.5	9
5	−Z	0.447	177.4	10	0.422	178.5	10
24	−Z	0.310	180.6	11	0.322	178.7	11
4	−Z	0.250	178.4	12	0.232	178.1	12
42	Y	0.185	2.7	13	0.172	359.1	13
41	−Z	0.153	183.8	14	0.155	180.1	14
3	−Z	0.137	178.5	15	0.129	178.6	15
5	−Y	0.112	183.0	16	0.112	181.0	16
242	−X	0.096	2.8	17	0.092	3.6	17
200	Y	0.079	2.3	18	0.073	3.5	19
241	−X	0.077	183.5	19	0.080	182.8	18
17	X	0.052	178.0	20	0.044	181.0	20
27	X	0.047	357.1	21	0.041	357.8	21
3	−Y	0.030	199.4	22	0.037	187.9	22
200	X	0.001	178.9	23	0.002	236.0	23

Table 3 Mode 4 comparison

Degree of freedom		External excitation			Active member excitation		
Grid	Dir.	Disp.	Phase	Order	Disp.	Phase	Order
242	−X	1.000	0.0	1	1.000	0.0	1
241	−X	0.963	180.3	2	0.962	182.1	2
3	−Y	0.927	355.9	3	0.961	4.7	3
200	Y	0.865	176.0	4	0.873	180.5	4
5	−Y	0.697	351.6	5	0.712	0.5	5
242	Z	0.497	276.2	6	0.151	38.4	13
142	Z	0.311	336.8	7	0.317	15.3	6
6	−Y−Z	0.283	344.6	8	0.277	356.7	7
41	−Z	0.283	210.0	9	0.239	186.3	9
42	Y	0.273	32.0	10	0.221	8.7	10
27	X	0.218	188.0	11	0.217	170.1	11
141	Z	0.210	133.2	12	0.178	173.3	12
27	Z	0.189	107.2	13	0.090	225.3	17
24	−Z	0.162	334.3	14	0.259	45.0	8
17	X	0.159	7.4	15	0.145	353.8	14
241	Z	0.110	269.4	16	0.064	86.4	21
203	——	0.095	215.9	17	0.070	190.3	19
17	Z	0.090	274.2	18	0.056	80.3	22
4	−Z	0.072	359.7	19	0.144	63.3	15
6	−Z	0.066	34.8	20	0.067	24.3	20
3	−Z	0.037	203.1	21	0.093	110.3	16
5	−Z	0.027	136.9	22	0.087	99.0	18
200	X	0.003	194.3	23	0.011	108.2	23

However, the response spectra of the midbay shaker mass and the midplate on which the shaker is located, as shown in Fig. 12, whose vertical scale is in milligrams, indicate that the three global mode responses are dominating. By normalizing the shaker mass response with respect to the midbay place response, strong resonance is evident at approximately 8.8 Hz, which is between the first and second global modes. Figure 13, whose vertical scale represents the ratio of the motions between the midbay shaker vs midbay plate, shows this result for both the external excitation and the diagonal active member excitation case. Basically, the normalizing procedure eliminates the rigid-body motion of the shaker mass with respect to the shaker, which is bolted to the midbay plate.

Local modes L2 and L3 are the outrigger mass rotation modes. During the curve fitting of the global modes, these two modes failed to converge due to low-level signals and high-

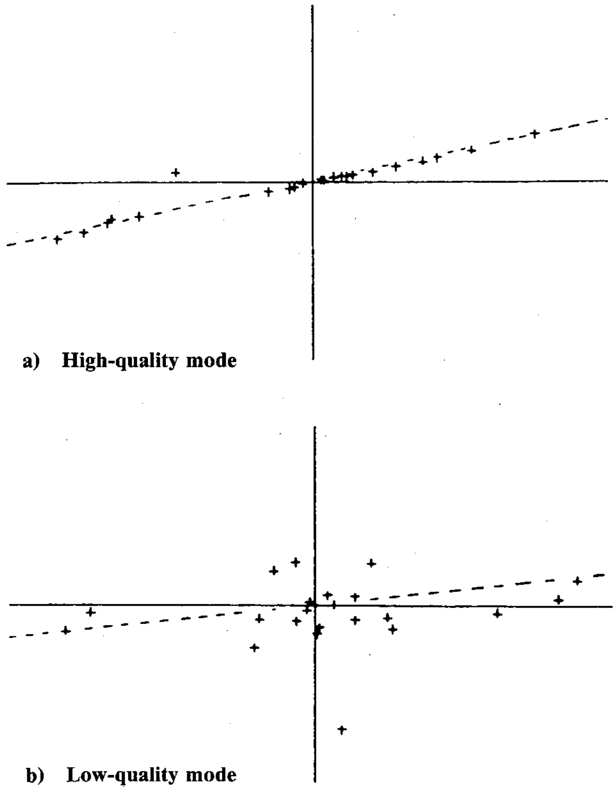

Fig. 9 Phase coherence criterion.

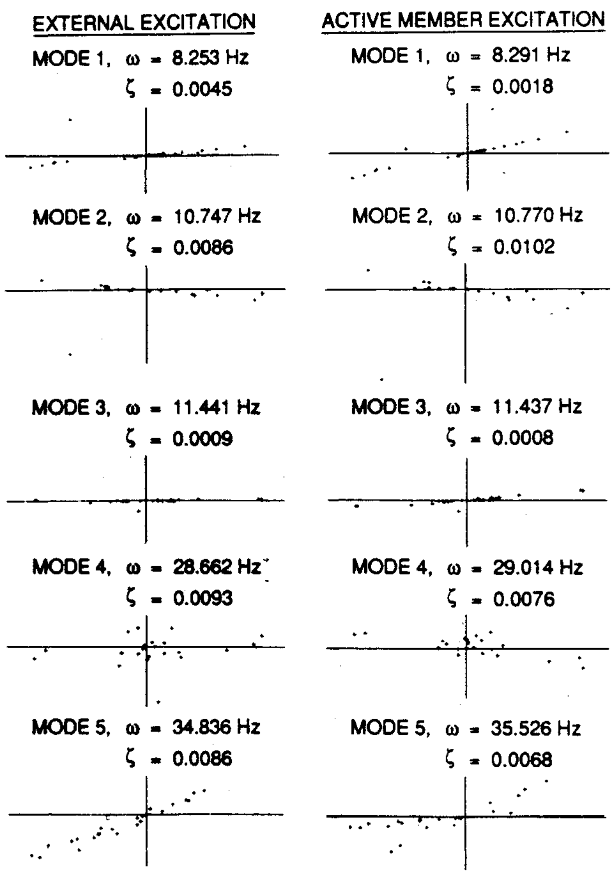

Fig. 10 Phase coherence for modes 1–5.

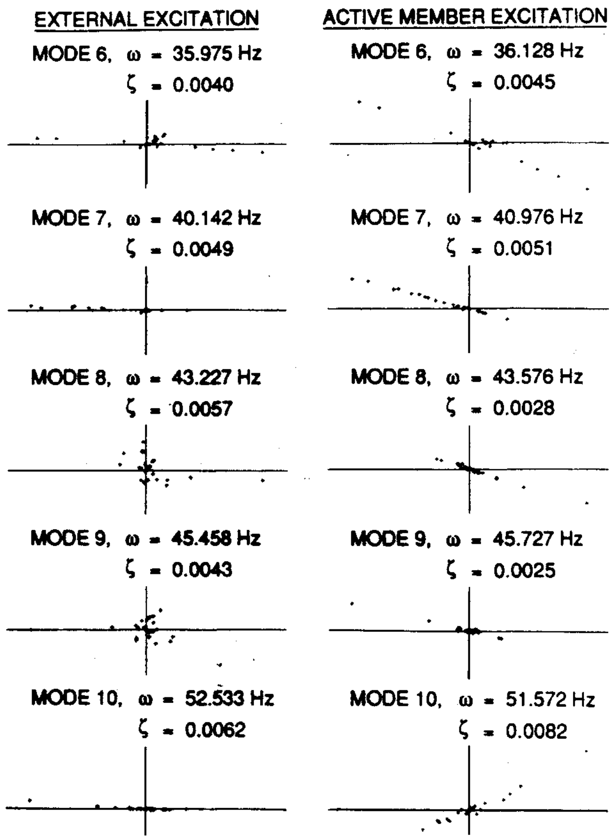

Fig. 11 Phase coherence for modes 6–10.

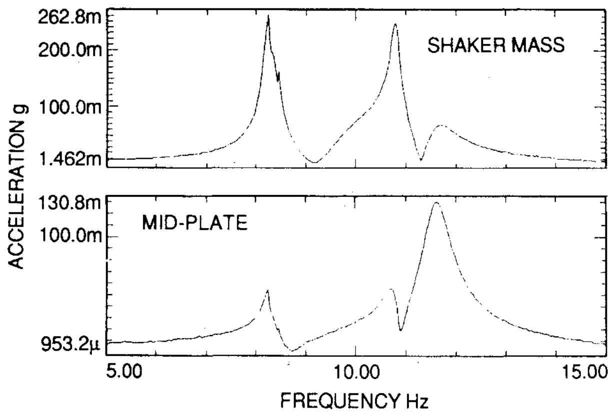

Fig. 12 Response spectra for local mode L1.

level noise in many of the channels except those on the outrigger masses. Figure 14, whose vertical scale is displacement in inches, shows the curve fittings for the four channels on the outrigger masses only. The modal parameters were extracted successfully from these channels alone and exhibited excellent phase coherence.

Active Member Measurements

Intuition tells one that the measurements of the displacement sensor and the load cell associated with the active member should be similar in their amplitudes as well as phase angles. Indeed, this is the case when the active member is not being used as the excitation source. Figure 15 shows such measurements from the nondriving active member strut 11 when the diagonal active strut is driving the structure. However, the measurements from a driving active member are different. Figure 16 shows several measurements from strut 22 when it is used as the excitation source. A constant voltage was recorded from the digital to analog converter (DAC). This signal is sent to the active member amplifier, and, again, a con-

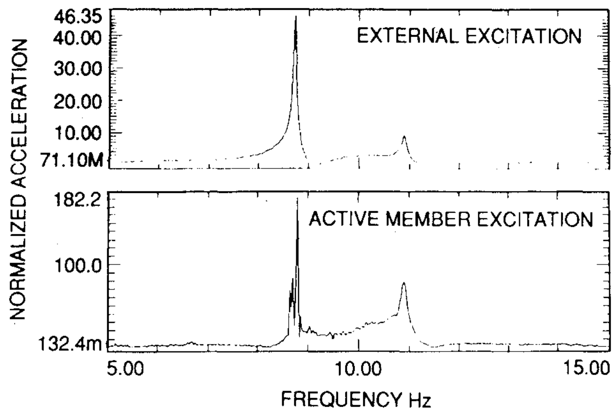

Fig. 13 Normalized response spectra for local mode L1.

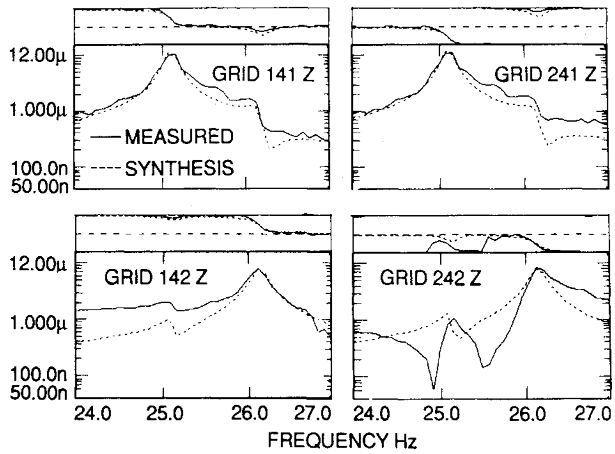

Fig. 14 Curve fittings for local modes L2 and L3.

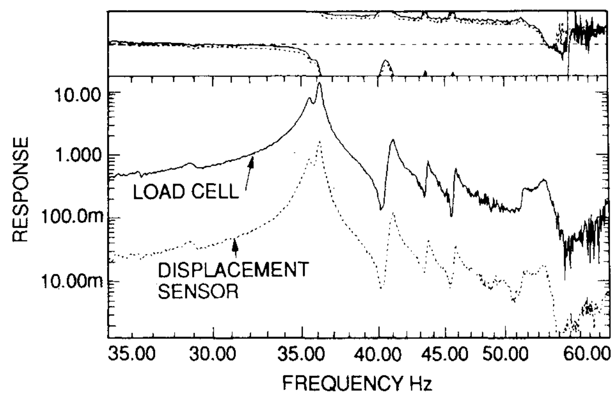

Fig. 15 Load cell and displacement sensor measurements for non-driving active member.

stant voltage was recorded as the output voltage to strut 22, which is the active member driving voltage. Theoretically, the force output from the active member as measured by the load cell and the displacement sensor measurement should be proportional to the driving voltage. But the actual measurements show slight fluctuations for the load cell and larger fluctuations for the displacement at the resonant frequencies. These measurements are plotted in different scales as shown in Fig. 17 to bring out the fluctuations. The reason is that the load cell and displacements measurements contain not only the input signal but also the structural responses particularly at the resonance. This is the reason that when frequency response functions are computed during the active member excitation the response spectra are divided by the driving voltage instead

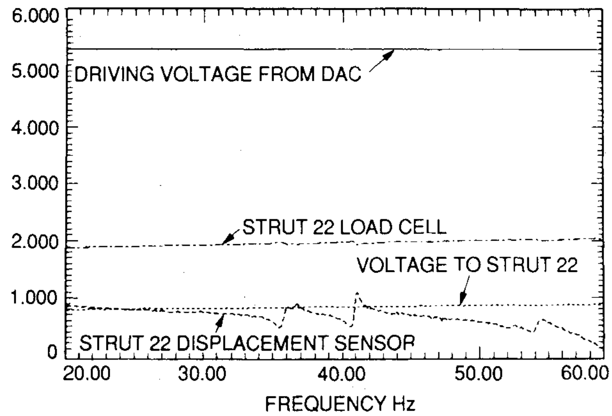

Fig. 16 Measurements of driving active member.

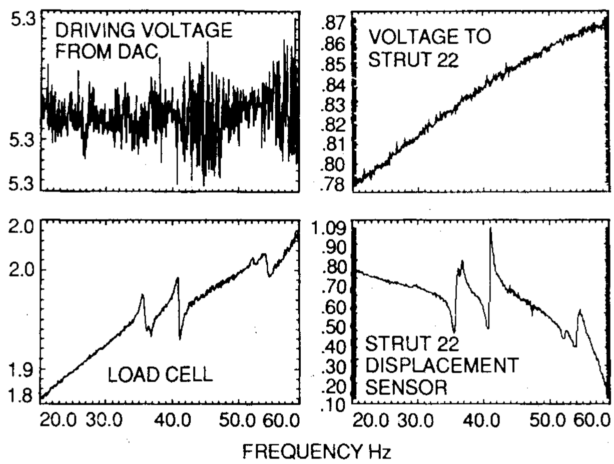

Fig. 17 Measurements of driving active member.

of the load cell force measurements. This is an important observation if any of the active member measurements are to be used in feedback control. Figures 15, 16, and 17 are intended to show the response profiles, not the amplitudes, of various measurements, therefore the vertical scales of these figures are arbitrarily set.

Damping Measurements

The curve-fitting procedure is not very sensitive to the extracted modal damping values. The somewhat large discrepancies among the obtained damping values could be due to the nature of the active members such as the hysteresis and creep with respect to the applied voltage shown in the test as well as due to the data processing. To assure that the estimated damping values are within the physical possibility, a sinusoidal decay test was performed. During the test, the structure was excited at the first three global frequencies by the diagonal active member and the power was suddenly cut off after a certain response level was achieved. The modal damping values are estimated based on the response decay, which is a physical phenomenon and should provide more accurate data. The results (not shown) were in agreement with most of the curve-fitting results. However, there were sufficient discrepancies such that further investigations are planned.

V. Concluding Remarks

The objective of the present study is to determine whether a modal test can be performed adequately using the active members as excitation sources. The results indicate that such a test can indeed produce modal parameters with equal or better accuracy as compared to those obtained by the conventional external excitation tests. This is an encouraging step that will further the development of on-orbit system identification tests for large space structures.

Acknowledgment

The research described in this paper was carried out by the Jet Propulsion Laboratory, California Institute of Technology, under NASA contract. This task was sponsored by Samuel L. Venneri, NASA Office of Aeronautics and Space Technology, Code RM.

References

[1]Canavin, J. R., "Control Technology for Large Space Structures," AIAA Paper 78-1691, April 1978.

[2]Chen, J.-C., "Response of Large Space Structures With Stiffness Control," *Journal of Spacecraft and Rockets,* Vol. 21, No. 5, 1984, pp. 463–467.

[3]Fanson, J. L., and Caughey, T. K., "Positive Position Feedback Control for Large Space Structures," AIAA Paper 87-0902, April 1987.

[4]Fanson, J. L., and Garba, J. A., "Experimental Studies of Active Members in Control of Large Space Structures," AIAA Paper 88-2207, April 1988.

[5]Forward, R. L., "Electronic Damping of Vibrations in Optical Structures," *Applied Optics*, Vol. 18, No. 5, 1979, pp. 690–697.

[6]Crawley, E. F., and De Luis, J., "Use of Piezoelectric Actuators as Elements of Intelligent Structures," *AIAA Journal*, Vol. 25, No. 10, 1987, pp 1373–1385.

[7]Natori, M., Motohashi, S., Takahara, K., and Kuwao, F., "Vibration Control of Truss Beam Structures Using Axial Force Actuators," AIAA Paper 88-2273, April 1988.

[8]Natori, M., Ogura, S., and Motohashi, S., "Vibration Control of Truss Structures Using Active Members," IAF-88-290, Oct. 1988, Bangalore, India.

[9]Onoda, J., Watanabe, N., Endo, T., and Tamaoki, H., "Vibration Suppression of Space Truss by Stiffness Control," International Astronautical Federation, Paper 89-334, Oct. 1989.

[10]Chen, J.-C., and Garba, J. A., "On-Orbit Damage Assessment for Large Space Structures," *AIAA Journal,* Vol. 26, No. 9, 1988, pp. 1119–1126.

[11]Fanson, J. L., Blackwood, G. H., and Chu, C. C., "Active-Member Control of Precision Truss," AIAA Paper 89-1329, April 1989.

[12]Chen, J.-C., "Evaluation of Modal Testing Methods," *Journal of Spacecraft and Rockets,* Vol. 24, No. 1, 1987, pp. 52–62.

[13]Chen, J.-C., and Wada, B. K., "Sine Dwell or Broadband Methods for Modal Testing," *AIAA Journal,* Vol. 26, No. 6, 1988, pp. 733–737.

[14]Hamma, G. A., Smith, S., and Stroud, R. C., "An Evaluation of Excitation and Analysis Methods for Modal Testing," Society of Automotive Engineers, Paper 760872, Oct. 1976.